Toxicology Letters 417 (2026) 111834

Contents lists available at ScienceDirect

Toxicology Letters

journal homepage: www.journals.elsevier.com/toxicology-letters

Transcript-protein discrepancy of glutamatergic receptor subunits in human iPSC-derived neurons: Implications for neurotoxicity testing

Melania Maria Serafini [a,*], Miriam Midali [a], Giacomo Grumelli [a], Alessandro Cutarelli [b], Marina Marinovich [a,c], Luciano Conti [b], Barbara Viviani [a,c]

[a] Department of Pharmacological and Biomolecular Sciences, "Rodolfo Paoletti", Università degli Studi di Milano, Milan, Italy
[b] Department of Cellular, Computational and Integrative Biology - CIBIO, Università degli Studi di Trento, Trento, Italy
[c] Center of Research on New Approach Methodologies (NAMs) in chemical risk assessment (SAFE-MI), Università degli Studi di Milano, Milan, Italy

ARTICLE INFO

Editor: Dr. Angela Mally

Keywords:
Human iPSC-derived Neurons
Neurotoxicology
NMDA Receptor
AMPA Receptor
Synaptogenesis
Transcript-protein Discrepancy

ABSTRACT

The development of robust human in vitro models is crucial for advancing neurotoxicology and reducing animal testing. Human-induced pluripotent stem cell (hiPSC)-derived neuronal models hold great promise, but still show limitations in recapitulating certain neurodevelopmental processes. Currently, rodent primary cultures remain the gold standard for studying complex processes such as synaptogenesis. A key mechanism in glutamatergic synapse maturation is the GluN2B/GluN2A switch, which promotes the recruitment of alpha-amino-3-hydroxy-5-methyl-4-isoxazolepropionic acid (AMPA) receptors, increasing the structural and functional complexity of the synaptic spines. This study characterizes the development of the glutamatergic machinery in hiPSC-derived neurons, focusing on the expression and maturation of N-methyl-D-aspartate (NMDA) and AMPA receptors. The increase of neuronal markers and the reduction of progenitor markers confirmed the differentiation efficiency. However, discrepancies emerged between transcriptional and protein profiles of key receptor subunits. GluN2A mRNA levels increased over time, while protein levels remained similar to those of neural progenitor cells (NPCs). Conversely, the GluN3A transcript increased at 30 and 60 days in vitro (DIV), while protein abundance decreased. Similar transcript–protein mismatches were observed for some AMPA receptor subunits. These results suggest that this model does not reach full glutamatergic maturity within the tested timeframe. Therefore, optimizing differentiation conditions (such as extending culture duration or adding maturation cues) may be necessary to better reproduce receptor dynamics. Finally, this study highlights the need to integrate protein-level analyses with transcriptional data to improve the reliability of hiPSC-derived neuronal models for neurotoxicity and NMDA receptor–mediated excitotoxicity studies.

1. Introduction

The transition away from animal-based research (Törnqvist et al., 2014; European Commission 2024; Poh and Stanslas, 2024), driven by the 3Rs principles (Russell and Burch, 1959) and supported by regulatory initiatives (European Union, 2010; FDA, 2025), has led to a growing emphasis on human-relevant in vitro models. In toxicology, the transition is moving faster (Grimm et al., 2023) through a combination of measures involving the Organization for Economic Co-operation and Development (OECD) and regulatory authorities. In the field of developmental neurotoxicity (DNT), this shift is exemplified by the OECD's development of the DNT in vitro battery (OECD, 2023), which includes assays targeting key neurodevelopmental processes. Disruptions caused by chemicals in these processes can potentially lead to harmful effects at the organ or whole-organism level (Rice and Barone, 2000; Rodier, 1994). An international panel of experts has critically assessed the currently available in vitro assays, concluding that several of them are sufficiently robust and reliable to support chemical screening and regulatory risk assessment (Bal-Price et al., 2018; Fritsche et al., 2017; Sachana et al., 2019). The assay collection is primarily based on cells of human origin. This is an advantage because it helps reduce uncertainties related to interspecies extrapolation. However, some assays still rely on rodent primary neurons (OECD, 2023), particularly the ones that mark neurite maturation, synaptogenesis, and neuronal network formation. This may be because, although the field is rapidly evolving with numerous protocols for generating different nervous system cell types

* Corresponding author.
E-mail address: melania.serafini@unimi.it (M.M. Serafini).

https://doi.org/10.1016/j.toxlet.2026.111834
Received 28 October 2025; Received in revised form 9 January 2026; Accepted 20 January 2026
Available online 25 January 2026

(Nimtz et al., 2020; Hirbec et al., 2020; Fritsche et al., 2021; Serafini et al., 2024; Telias, 2023; Tal et al., 2024), human-derived neuronal models still face limitations in fully recapitulating these complex phenomena at the robustness and reproducibility levels required for standardized screening (Barral and Kurian, 2016; Mateos-Aparicios et al., 2020; Berryer et al., 2023; OECD, 2023).

Rodent primary neurons have long served as the gold standard for studying these processes (Banker and Goslin, 1998; Kaech and Banker, 2006), particularly synapse formation and synaptic spine dynamics, due to their robustness, rapid development, and reproducibility. However, human-derived models are being increasingly explored to overcome interspecies limitations and enhance translational relevance (OECD, 2023; Odawara et al. 2016). Synaptogenesis is a key neurodevelopmental process essential for establishing functional neural networks and precise brain circuitry (Cohen-Cory, 2002). The NMDA receptor (NMDAR) plays a fundamental role in both early and late phases of synaptogenesis in excitatory neurons, contributing to the maturation of glutamatergic synapses (Paoletti et al., 2013). During development, a switch from GluN2B-containing NMDA receptors, which are predominant in early life, to GluN2A-containing receptors, which are predominant in adulthood, occurs (Yasuda and Mukai, 2015; Hamada et al., 2014). This process is crucial for synaptic maturation and plasticity (Shipton and Paulsen, 2013) as it alters the kinetics, trafficking, and downstream signalling of receptors (Storey et al., 2025). Disruptions to the timing or extent of this transition have been associated with the pathophysiology of various neurodevelopmental disorders, including autism spectrum disorder and intellectual disability (Burnashev and Szepetowski, 2015; Uzunova et al., 2014). Imbalances in excitatory neurotransmission resulting from aberrant GluN2 subunit composition can affect critical periods of brain development, ultimately contributing to the manifestation of these conditions. The developmental switch from GluN2B to GluN2A subunits occurs both in vivo and in vitro (Williams et al., 1993). Rat primary hippocampal neurons, for example, closely reflect these developmental molecular dynamics of the glutamatergic system, with changes in NMDAR distribution observed during maturation (Rao and Craig, 1997). To date, the temporal and functional dynamics of the GluN2B/GluN2A switch remain poorly characterized in human iPSC-derived neurons, raising questions about their accuracy in modeling NMDAR maturation. To address this gap, and given the crucial role of NMDARs and AMPARs in synaptogenesis and neuronal function, this study aims to characterize the glutamatergic machinery in the human neural precursor cells (hNPCs)-derived neuronal model recently proposed by Romito and colleagues (Romito et al. 2024).

2. Materials and methods

2.1. hiPSCs maintenance and neural induction

HiPSCs were purchased from ThermoFisher Scientific. The cells were cultured and reprogrammed into neural progenitor cells (NPCs) using a monolayer neural induction procedure according to the instructions of a commercial kit (A1647801; ThermoFisher Scientific, Waltham, MA, US), as Romito and colleagues previously described (Romito et al. 2024).

2.2. hNPCs differentiation

hNPCs were plated in 5 µg/mL Laminin-coated (23017-015; Gibco, ThermoFisher Scientific, Waltham, MA, US) plastic supports maintained at 37°C, 5 % CO_2. Cell density was set at 2,6 × 10^4 cells/cm^2. For hNPCs neuronal differentiation, cultures were exposed to Neurobasal medium (21103-049; Gibco, ThermoFisher Scientific, Waltham, MA, US) supplemented with 1 % GlutaMAX (35050-061; Gibco), 1 % Pen-Strep (ECB3001D; Euroclone, Pero, Italy), 1 % non-essential amino acids (M7145–mL; Sigma-Aldrich, Merck KGaA, Darmstadt, Germany), 1 % B-27 Supplement (17504-044; Gibco, ThermoFisher Scientific, Waltham, MA, US) 1 % N2 supplement (17502-048; Gibco, ThermoFisher Scientific, Waltham, MA, US), 200 µM Ascorbic Acid (A92902; Sigma-Aldrich, Merck KGaA, Darmstadt, Germany), 1 µM Dibutyrryl cyclic AMP (db-cAMP; D0627; Sigma-Aldrich, Merck KGaA, Darmstadt, Germany) and 10 ng/mL BDNF (GFHA1F-100; Cell Guidance Systems, Babraham, Cambridge, UK). On the first day of differentiation, rock inhibitor 10 µM (Y-27632; 281642A; ChemCruz, Dallas, TX, US) was added to the medium. Half of the medium volume was changed twice a week until the desired time point (5, 15, 30, 60 days in vitro - DIV).

2.3. Immunofluorescence staining

Cells on coverslips were fixed with 4 % paraformaldehyde for 15 min at RT. Then, coverslips were washed with PBS, and cells were permeabilized with 0.1 % Triton X-100 in PBS for 15 min at RT. The blocking of the non-specific sites was performed by incubating coverslips for 1 h at RT with 5 % bovine serum albumin (BSA) in PBS. Cells were then stained with primary antibody diluted in 5 % BSA overnight at 4°C in a dark, humidified chamber. The day after, cells were washed 3 times with PBS and incubated with fluorophore-conjugated secondary antibody diluted in 5 % BSA for 1 h at RT in a dark, humidified chamber. Antibody details are listed in Section 2.7. Finally, cells were washed 3 times with PBS, protected from light, and mounted with Vectashield mounting medium with DAPI (H-1200, Vector Laboratories, Newark, CA, US). Slides were stored at 4°C until image acquisition. The images were acquired with a Zeiss Axio Observer Z1 microscope (40x oil-immersion objective).

2.4. SOX1 and SOX2 nuclear localization

Fixed cells were stained as described in Section 2.3. All the images were acquired with a Zeiss Axio Observer Z1 microscope (40x oil-immersion objective). The range indicator tool was used to monitor and avoid signal saturation. The number of SOX1- and SOX2-positive cells was quantified and normalized to the total number of cells in the field, as determined by DAPI staining.

2.5. RNA extraction and quantitative reverse transcriptase-polymerase chain reaction (RT-qPCR)

Total RNA was extracted from 1.5 × 10^6 cells following the instructions of TRIzol® reagent (Invitrogen Corporation, Carlsbad, CA, USA). Two µg of total RNA was retrotranscribed with QuantiTect reverse transcription kit (Qiagen, Valencia, CA, USA) following the manufacturer's instructions. Gene expression analysis was performed using QuantiTect SYBR Green PCR kit (Qiagen, Valencia, CA, USA). Human QuantiTect Primer Assays (Qiagen, Valencia, CA, USA) for the following genes: NES, PAX6, SOX1, SOX2, TUBB3, GFAP, MAP2, GRIN1, GRIN2A, GRIN2B, GRIN2C, GRIN2D, GRIN3A, GRIA1, GRIA2, GRIA3, GRIA4, and 18 s were used. The choice of 18 s as the housekeeping gene was performed by evaluating the expression stability of 3 different candidate reference genes using two popular algorithms: BestKeeper (Pfaffl et al., 2004) and NormFinder (Andersen et al., 2004).

2.6. Western blotting

The total homogenate (HOMO) of the hNPCs was prepared using a glass-glass potter in ice-cold lysis buffer (sucrose 0.32 M, Hepes 1 mM, $MgCl_2$ 1 mM, 150 $NaHCO_3$ 1 mM, PMSF 0.1 mM, at pH 7.4) supplemented with cocktails of proteases (Roche Diagnostics, Basel, Switzerland) and phosphatases inhibitors (Sigma-Aldrich, Merck KGaA, Darmstadt, Germany). The amount of protein in each sample was measured through the Bradford assay. The samples were prepared by dilution in sample buffer (62.5 mM Tris/HCl pH 6.8, 2 % SDS, 10 % glycerol, 5 % 2-mercaptoethanol, and bromophenol blue) and

denaturation by boiling for 10 min at 95°C. In each gel lane, 30 μg of proteins were loaded and separated in a denaturing sodium dodecyl-sulfate polyacrylamide gel electrophoresis (SDS-PAGE). Proteins were then blotted onto nitrocellulose membranes. Then, membranes were blocked in I-block solution (Tris-buffered saline, 1 % Tween 20, TBS-T) for 1 h at room temperature on a shaker. After the blocking of the aspecific sites, membranes were incubated with primary antibodies diluted in I-block. The incubation was performed overnight at 4°C. The day after, membranes were washed 3 times with TBS-T and subsequently incubated with the horseradish peroxidase (HRP)-conjugated secondary antibody diluted in I-block for 1 h at RT. At the end of incubation and after 3 additional washes with TBS-T, protein signals were detected through enhanced chemiluminescence (ECL) reagents and the use of a Chemidoc (Bio-Rad, Hercules, CA, USA). The relative optical density (OD) was measured using Image Lab Software (Bio-Rad, Hercules, CA, USA).

2.7. Reagents and antibodies

Information about primary and secondary antibodies is presented in Table 1 and Table 2.

2.8. Statistical analysis

The statistical analyses were performed using GraphPad PRISM software (version 10.2). All data are expressed as mean ± SEM. The number of replicates is reported in the figure legends. For group comparisons, unpaired two-tailed Student's *t*-test or one-way ANOVA, followed by Tukey or Dunnett post hoc tests, were used. The value of $p < 0.05$ was considered statistically significant. Before statistical analysis, outliers were removed (a maximum of 1 for each dataset) using a standard deviation (SD) criterion. Values with SD from the mean greater than ±2.5 were discarded.

Table 1
Primary antibodies details. Protein targets, brands, product codes, applications, and working dilutions are reported. WB: Western Blotting; IF: Immunofluorescence.

Target	Brand	Product Code	Dilution
Anti-Nestin	Invitrogen	A24345	1:50 (IF)
Anti-SOX2	Invitrogen	A24339	1:50 (IF)
Anti-SOX1	Invitrogen	A24347	1:50 (IF)
Anti-PAX6	Invitrogen	A24340	1:50 (IF)
Anti-MAP2	Abcam	ab5392	1:500 (IF)
Anti-β-III-Tubulin	Invitrogen	PA5–85639	1:500 (IF) 1:1000 (WB)
Anti-Synaptophysin	Cell Signaling Technology	D8F6H	1:250 (IF)
Anti-PSD95	Cell Signaling Technology	7E3	1:250 (IF)
Anti-GFAP	Cell Signaling Technology	D1F4Q	1:1000 (WB)
Anti-GluN1	Invitrogen	32–0500	1:1000 (WB)
Anti-GluN2A	Sigma-Aldrich	M264	1:1000 (WB)
Anti-GluN2B	Cell Signaling Technology	D8E10	1:1000 (WB)
Anti-GluN2C	Biorbyt	Orb215473	1:1000 (WB)
Anti-GluN2D	Biorbyt	Orb539724	1:1000 (WB)
Anti-GluN3A	Millipore	07–356	1:1000 (WB)
Anti-GluA1	Cell Signaling Technology	D4N9V	1:1000 (WB)
Anti-GluA2	Neuromab	75–002 clone L21/32	1:1000 (WB)
Anti-GluA3	Cell Signaling Technology	D47E3	1:1000 (WB)
Anti-GluA4	Cell Signaling Technology	D41A11	1:1000 (WB)
Anti-Actin	Sigma Aldrich	A5441	1:2500 (WB)

Table 2
Secondary antibodies details. Conjugations, fluorophores, brands, product codes, applications, and working dilutions are reported. WB: Western Blotting; IF: Immunofluorescence.

Target	Brand	Product Code	Dilution
HRP-Conjugated anti-mouse	Bio-Rad	172–1011	1:10,000 (WB)
HRP-Conjugated anti-rabbit	Bio-Rad	172–1019	1:10,000 (WB)
HRP-Conjugated anti-chicken	Invitrogen	A16054	1:10,000 (WB)
AlexaFluor 488-conjugated anti-goat	Life Technologies	A24349	1:250 (IF)
AlexaFluor 488-conjugated anti-mouse	Life Technologies	A24350	1:250 (IF)
AlexaFluor 555-conjugated anti-rabbit	Life Technologies	A24342	1:250 (IF)
AlexaFluor 488-conjugated anti-chicken	Invitrogen	A11039	1:500 (IF)

3. Results

3.1. hNPCs differentiation

To monitor the progression of hNPC differentiation, four key markers were analyzed at 0, 5, 15, 30, and 60 DIV: sex-determining region Y (SRY)-related HMG box 1 and 2 (SOX1 and SOX2), the paired box protein (PAX6), and the neuroepithelial stem cell protein (Nestin). These markers are commonly associated with neural progenitor identity and are expected to decrease as differentiation progresses.

To quantitatively assess the progression of hNPC differentiation, mRNA expression levels of Nestin, SOX1, SOX2, and PAX6 were analyzed by RT-qPCR at 0, 30, and 60 DIV. A significant downregulation of Nestin (Fig. 1C), SOX1 (Fig. 1E), and SOX2 (Fig. 1F) were observed at 30 and 60 DIV compared to undifferentiated hNPCs (0 DIV). PAX6 (Fig. 1D) also showed a decreasing trend, although without reaching statistical significance, likely due to high data dispersion. To further quantify protein-level changes, co-localization analysis of SOX1 (Fig. 1G) and SOX2 (Fig. 1H) with the fluorescent nuclear probe 4′,6-diamidino-2-phenylindole (DAPI) was performed. This analysis confirmed a marked reduction in SOX1- and SOX2-positive cells at 30 and 60 DIV, supporting the RT-qPCR findings. These quantitative analyses provide robust evidence of the downregulation of progenitor markers during differentiation. This trend is further supported by complementary immunofluorescence staining, which revealed a progressive decrease in Nestin and SOX2 protein levels (Fig. 1A), as well as SOX1 and PAX6 (Fig. 1B). Furthermore, Nestin staining, the only cytoplasmic protein analyzed in this first panel, allows visualization of progressive changes in cell morphology during neuronal differentiation over the days in vitro.

At the same time points, the known markers of neuronal differentiation, Microtubule-Associated Protein 2 (MAP2) and β-III-Tubulin, were analyzed. To quantitatively assess neuronal differentiation, the expression of β-III-tubulin and MAP2 was analyzed by RT-qPCR and Western blot. The gene encoding β-III-tubulin showed a significant increase at 15 and 30 DIV compared to hNPCs (0 DIV), with no further changes between 30 and 60 DIV (Fig. 2C). Western blot analysis confirmed a significant increase in β-III-tubulin protein levels at 30 and 60 DIV (Fig. 2F). For MAP2, RT-qPCR revealed a progressive upregulation during differentiation, with a statistically significant increase at 30 DIV compared to hNPCs (Fig. 2E). These quantitative findings were

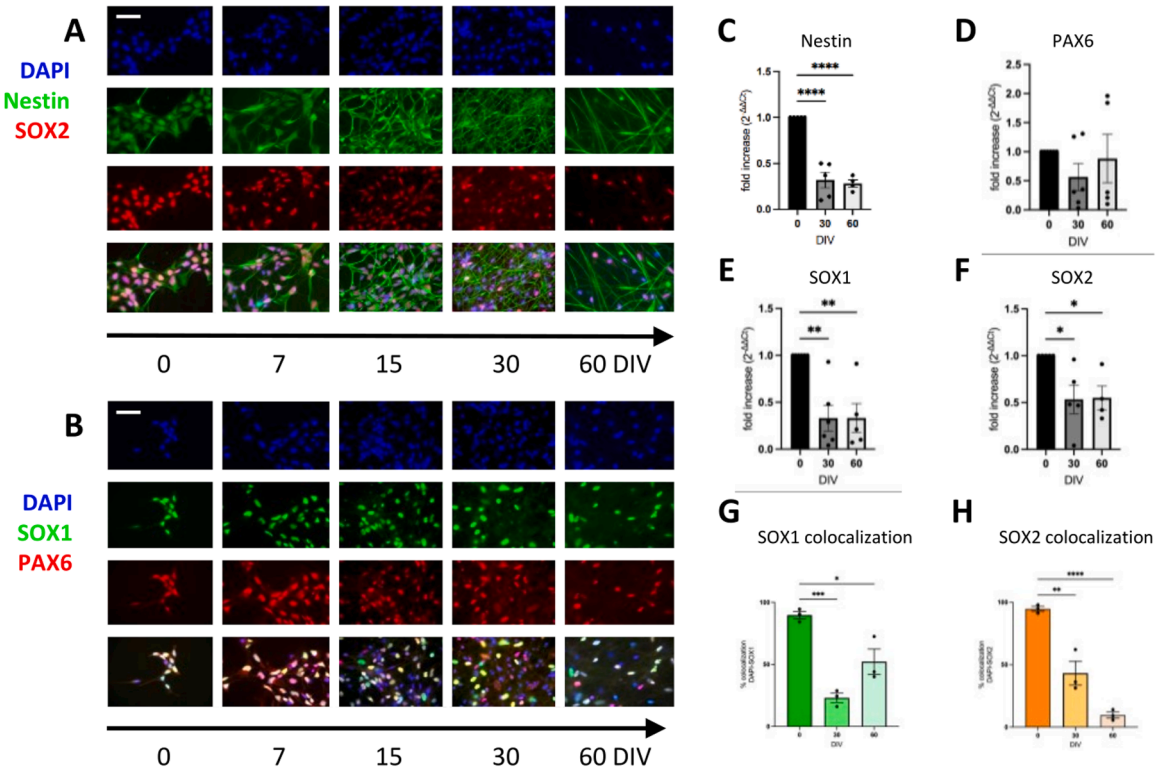

Fig. 1. hNPCs differentiation into neurons - stem cell markers. Representative images of immunofluorescence staining of Nestin-SOX2 (A) and SOX1-PAX6 (B) at different time points of hNPCs differentiation (0, 7, 15, 30, 60 DIV). Scale bar 50 μm. DAPI was used to stain cell nuclei. QRT-PCR analysis of mRNA levels of genes coding for Nestin (C), PAX6 (D), SOX1 (E), and SOX2 (F) during hNPCs differentiation at 0, 30, and 60 DIV. Data are expressed as mean ± SEM ($n \geq 4$) of relative fold gene expression calculated with the $2^{-\Delta\Delta Ct}$ method. Quantitative analysis of SOX1- (G) and SOX2- (H) positive cells at 0, 30, and 60 DIV. Data are expressed as % of SOX1 or SOX2 immunoreactive cells. Data are expressed as mean ± SEM ($n = 3$). One-way ANOVA followed by Dunnett's post-hoc test * $p < 0.05$; ** $p < 0.01$; *** $p < 0.001$; **** $p < 0.0001$.

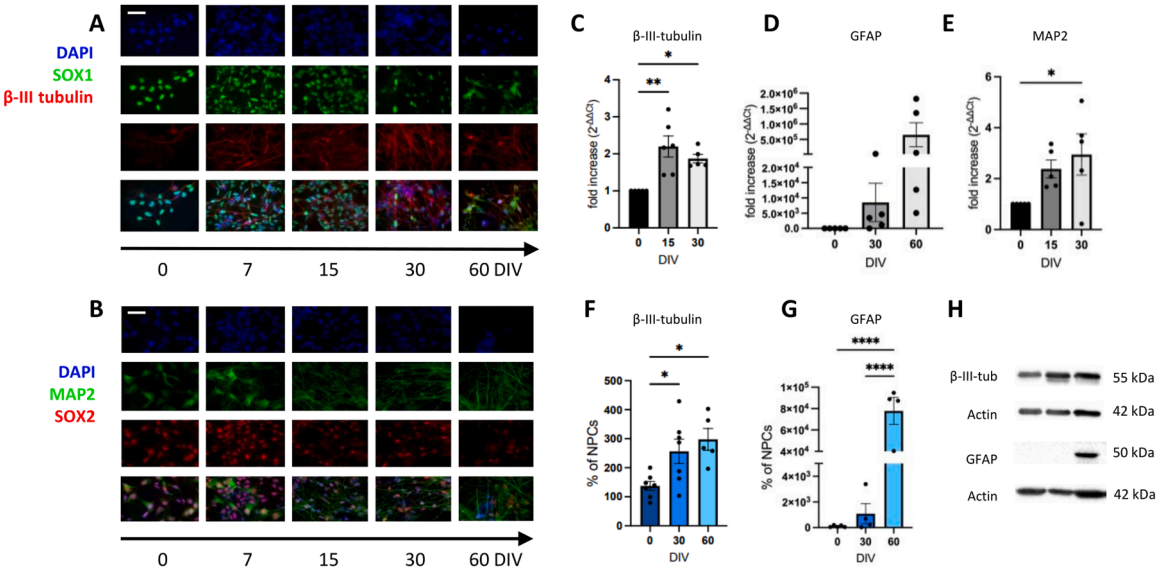

Fig. 2. hNPCs differentiation into neurons - neuronal and glial markers. Representative images of immunofluorescence staining of β-III-tubulin/SOX1 (A) and MAP2/SOX2 (B) at different time points of hNPCs differentiation (0, 7, 15, 30, 60 DIV). Scale bar 50 μm. DAPI was used to stain cell nuclei. QRT-PCR analysis of mRNA levels of genes coding for β-III-tubulin (C), and MAP2 (E) during hNPCs differentiation at 0, 15, and 30 DIV, and for GFAP (D) at 0, 30, and 60 DIV. Data are expressed as mean ± SEM ($n \geq 5$) of relative fold gene expression calculated with the $2^{-\Delta\Delta Ct}$ method. Western blot analysis of β-III-tubulin (F) and MAP2 (G) during hNPCs differentiation at 0, 30, and 60 DIV. Protein levels were normalized to actin and expressed as % of NPCs (0 DIV). Data are expressed as mean ± SEM ($n \geq 4$). Representative western blot images (H). One-way ANOVA followed by Dunnett's post-hoc test * $p < 0.05$; ** $p < 0.01$; **** $p < 0.0001$.

supported by immunofluorescence staining. β-III-tubulin was barely detectable at 0 DIV and weakly expressed at 7 DIV, but its signal intensified from 15 DIV onward, forming a complex neuronal network by 30 DIV (Fig. 2A). MAP2 showed a distinct pattern: it was already

present in the cytoplasm at 0 DIV, and from 15 DIV, the signal adopted a filamentous distribution, reflecting the morphological transition of hNPCs into elongated, polarized neurons (Fig. 2B).

Together with markers of neuronal differentiation, we checked for the presence of GFAP, a protein expressed in the CNS in astrocyte cells (Li et al. 2020). RT-qPCR data revealed that hNPCs had also differentiated into glial cells (Fig. 2D) since a trend of increased mRNA expression was detected at 30 and 60 DIV. This data was strengthened by western blot analysis showing that GFAP protein abundance is enhanced at 60 DIV versus both hNPCs (0 DIV) and 30 DIV (Fig. 2G).

3.2. Transcript levels of genes coding for the main subunits of NMDA and AMPA receptors

For mRNA expression analysis of the glutamatergic machinery, we focused on a single time point (30 DIV) because our previous assessment of neuronal differentiation markers did not reveal significant differences between 30 and 60 DIV. In addition, we observed an increase in astrocytic markers (i.e., GFAP) at 60 DIV. In line with our neurocentric approach, we conducted experiments at 30 DIV to minimize the contribution of glial cells and mitigate the interference of astrocytes, whose known expression of glutamate receptors could confound our analysis (Belachew and Gallo, 2004; Verkhratsky and Chvátal, 2020; Kosenkov et al., 2024). The mRNA levels of genes coding for the main subunits of NMDA and AMPA receptors were assessed. Of the 6 NMDA receptor subunits analyzed, increased levels of GRIN2A, GRIN2B, GRIN2D, and GRIN3A (Fig. 3B, C, E, and F) were found at 30 DIV compared to hNPCs at 0 DIV. For the GRIN1 subunit, an increasing trend at 30 DIV compared to 0 DIV was found, although not significant, possibly due to high data dispersion (Fig. 3A). For the GRIN2C subunit, there was no significant change over time (Fig. 3D).

As for AMPA receptor subunit gene expression, increased levels of GRIA2 and GRIA4 (Fig. 4B and D) were found at 30 DIV compared to hNPCs at 0 DIV. While for the GRIA1 and GRIA3 subunits, there was no significant change over time (Fig. 4A and C).

3.3. Protein abundance of the main subunits of NMDA and AMPA receptors

The protein abundance of the major subunits of NMDA and AMPA receptors was assessed at two time points: at 30 DIV for comparison with the mRNA results, and at 60 DIV to investigate a more mature developmental stage. For GluN1 and GluN2A, no differences were found between 0, 30, and 60 DIV, but an increase (for GluN1) and decreasing (for GluN2A) trends were observed (Fig. 5A and B). GluN2B protein abundance was found to be significantly increased at 30 and 60 DIV compared to hNPCs at 0 DIV (Fig. 5C). A trend of increase was found for GluN2C (Fig. 5D), although not significant, possibly due to high data dispersion. On the contrary, the GluN2D subunit showed a trend of decrease over time (Fig. 5E), and GluN3A protein abundance significantly decreased during differentiation, at 30 and 60 DIV, compared to hNPCs at 0 DIV (Fig. 5F). There was no statistically significant difference between 30 and 60 DIV for any of the subunits analyzed.

As for AMPA receptor expression, a time-dependent trend of increase was found for GluA1 (Fig. 6A). The GluA2 subunit showed a trend of increase at 30 DIV compared to hNPCs, although the levels at 60 DIV showed a trend of decrease, with levels similar to those at 0 DIV (Fig. 6B). The GluA3 and GluA4 subunits were significantly increased, respectively, at 60 and 30 DIV of differentiation compared to hNPCs at 0 DIV (Fig. 6C and D).

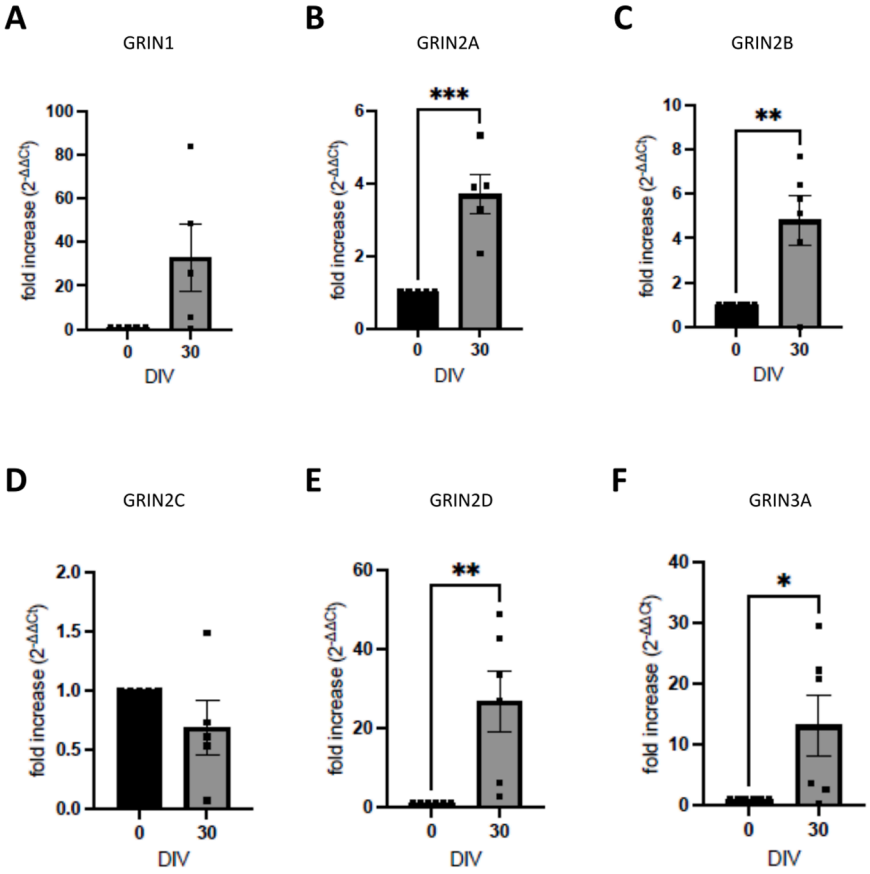

Fig. 3. mRNA levels of the main NMDA receptor subunits. RNA from total cellular extracts of 30 DIV differentiated hNPCs was analyzed for GRIN1 (A), GRIN2A (B), GRIN2B (C), GRIN2C (D), GRIN2D (E), and GRIN3A (F) mRNA expression by qRT-PCR. 18 s was used as the housekeeping gene. Data are expressed as mean ± SEM ($n \geq 5$) of relative fold gene expression calculated with the $2^{-\Delta\Delta Ct}$ method. Unpaired two-tailed Student's *t*-test, * $p < 0.05$; ** $p < 0.01$; *** $p < 0.001$.

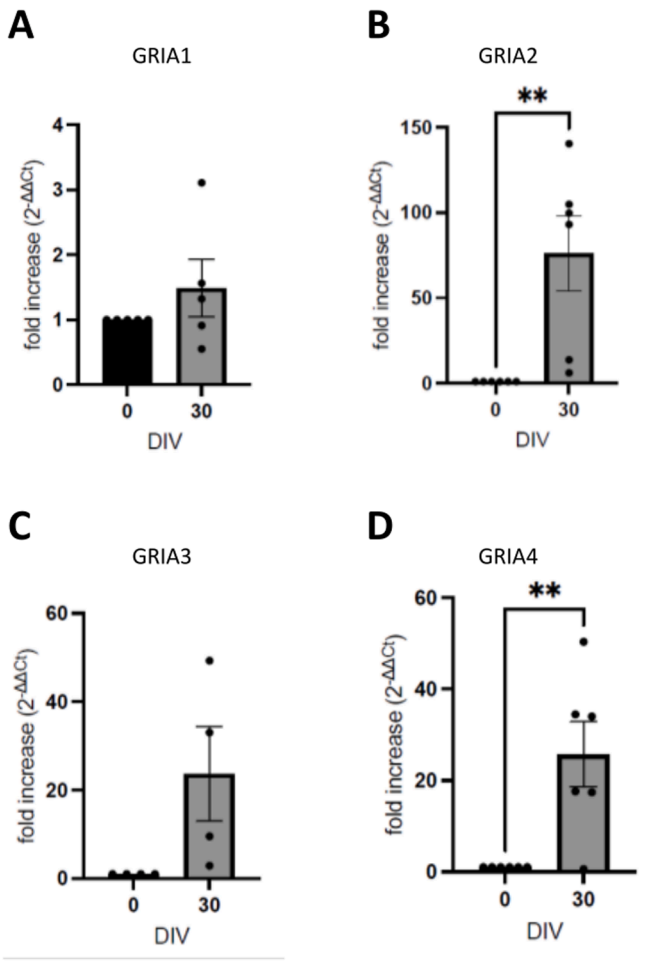

Fig. 4. mRNA levels of the AMPA receptor subunits. RNA from total cellular extracts of 30 DIV differentiated hNPCs was analyzed for GRIA1 (A), GRIA2 (B), GRIA3 (C), and GRIA4 (D) mRNA expression by RT-qPCR. 18 s was used as the housekeeping gene. Data are expressed as mean ± SEM ($n \geq 5$) of relative fold gene expression calculated with the $2^{-\Delta\Delta Ct}$ method. Unpaired two-tailed Student's *t*-test, ** $p < 0.01$.

To complement the molecular analysis of glutamatergic receptor subunits, synaptic organization was evaluated by immunofluorescence staining of the pre-synaptic marker synaptophysin and the post-synaptic marker PSD95 at 30 and 60 DIV (Supplementary Figure 1). At both time points, staining appeared diffuse and did not display the punctate pattern typically associated with the formation of synaptic contacts.

4. Discussion

hNPCs differentiation is a complex, multistep process orchestrated by several transcription factors (Singh et al., 2023). We monitored hNPC differentiation by analyzing the time-dependent expression of key progenitor markers. SOX1 and SOX2 are members of the SOXB1 family of transcription factors, which are central regulators of neurodevelopment. SOX1 is one of the earliest markers of neuroectodermal commitment (Pevny et al., 1998), while SOX2 is essential for stem cell maintenance in the CNS and is broadly expressed in undifferentiated neural cells (Amador-Arjona et al., 2015). PAX6 plays a dual role in embryonic and adult neurogenesis, contributing to the maintenance of the NSC pool (Sansom et al., 2009). Nestin is typically restricted to progenitor cells and is downregulated upon neuronal commitment (Bernal and Arranz, 2018). The decrease in these markers supports the successful transition from a progenitor to a more differentiated neuronal state. These findings align with previous reports on the temporal dynamics of transcription factor expression during neurogenesis (Wegner and Stolt, 2005). The differentiation protocol we adopted successfully generated neurons, as demonstrated by the upregulation of neuronal markers MAP2 and β-III-tubulin. These are well-established indicators of neuronal identity (Marei et al., 2018): MAP2 is predominantly expressed in dendrites (Harada et al., 2002), while β-III-tubulin is mainly localized in axons (Niwa et al., 2013). The detection of glial cell marker (i.e., GFAP) at 30 DIV and its increase at 60 DIV revealed the possible presence of glial cells (i.e., astrocytes). This dynamic is consistent with previous evidence reporting an increased expression of the astrocytic marker GFAP as early as 30 DIV (Szabo et al., 2021). These findings confirm that the in vitro model follows the expected differentiation trajectory described by Romito et al. (2024).

Despite successful differentiation, the analysis of ionotropic glutamatergic receptors revealed a discrepancy between mRNA and protein levels, especially for NMDAR subunits. NMDARs are heterotetrameric receptors. Two GluN1 subunits are required for proper assembly along with two modulatory subunits. These modulatory components are encoded by four *grin2* genes (GluN2A-D) and two *grin3* genes (GluN3A and GluN3B) (Vyklicky et al., 2014), and their specific combination determines the receptor's physiological and pharmacological characteristics (Paoletti et al., 2013). A previous study conducted under feeder-free conditions revealed that *grin1* mRNA was undetectable in NPCs and only appeared in differentiated neurons, peaking at 45 days in vitro (DIV) (Baldassari et al., 2022). A similar trend was also reported by Cheng and colleagues, who found that *grin1* mRNA levels tend to increase at 4 and 6 weeks, although with high variability (Cheng et al., 2024). In line with these studies, we found that *grin1* mRNA increased over time in our system. However, our data showed no difference in GluN1 protein levels between NPCs and 30 DIV-differentiated neurons, though we did observe a trend toward increased levels at 60 DIV. Single-cell RNA sequencing on iPSC-induced glutamatergic neurons at 28 DIV shows that the expression of *grin1* and *grin2a* mRNA is markedly lower than that of *grin2b*. In this study, no data are available to evaluate the mRNA temporal expression pattern (Gameiro-Ros et al., 2025), and the authors did not measure protein levels. These data, together, suggest that a longer differentiation period might enhance GluN1 protein abundance, which is often considered an indicator of functional neuronal maturation. NMDAR subunit composition is known to change over development. The expression of the different subunits is tightly regulated, and this regulation occurs in a specific temporal pattern that coincides with synapse maturation (Gambrill and Barria, 2011). This refers particularly to the subunits GluN2A and GluN2B in the hippocampus and cortical areas (Williams et al., 1993) and has been demonstrated not only in animal models, but also in human brains (Bar-Shira et al., 2015). During maturation, GluN2A expression increases while GluN2B predominates in immature neurons (Sanz-Clemente et al., 2013), making their ratio a hallmark of synaptic development (Paoletti et al., 2013). Findings in shGluN2A-transduced neurons showed that the reduction in GluN2A in hippocampal cultures induces an imbalance in the GluN2A/GluN2B ratio, which reflects a more immature phenotype (Acutain et al., 2021). In rodent models, the failure of the subunit switch has been associated with impaired synaptic plasticity and neurodevelopmental phenotypes (Shipton and Paulsen, 2013). Similarly, the disruption in temporal and spatial NMDARs dynamics in humans is linked to neurodevelopmental disorders (Tumdam et al., 2024), while human GRIN2A mutations lead to deficits in receptor trafficking and function (Addis et al., 2017; Vieira et al., 2020; Yong et al., 2021; Vieira et al., 2024). A recent study in iPSC-derived cortical neurons reports that the mRNA levels of GluN2A and GluN2B follow a similar trend, both peaking at 4 weeks (Cheng et al., 2024). These data are consistent with our observations of an increase in both transcripts at 30 DIV (~4 weeks). The human mixed cortical neurons obtained by Klima and colleagues showed an increase in mRNA expression from 10 to 21 DIV, with a similar trend for all three analyzed subunits (*grin1*, *grin2a*, and *grin2b*) (Klima et al., 2021). A separate publication

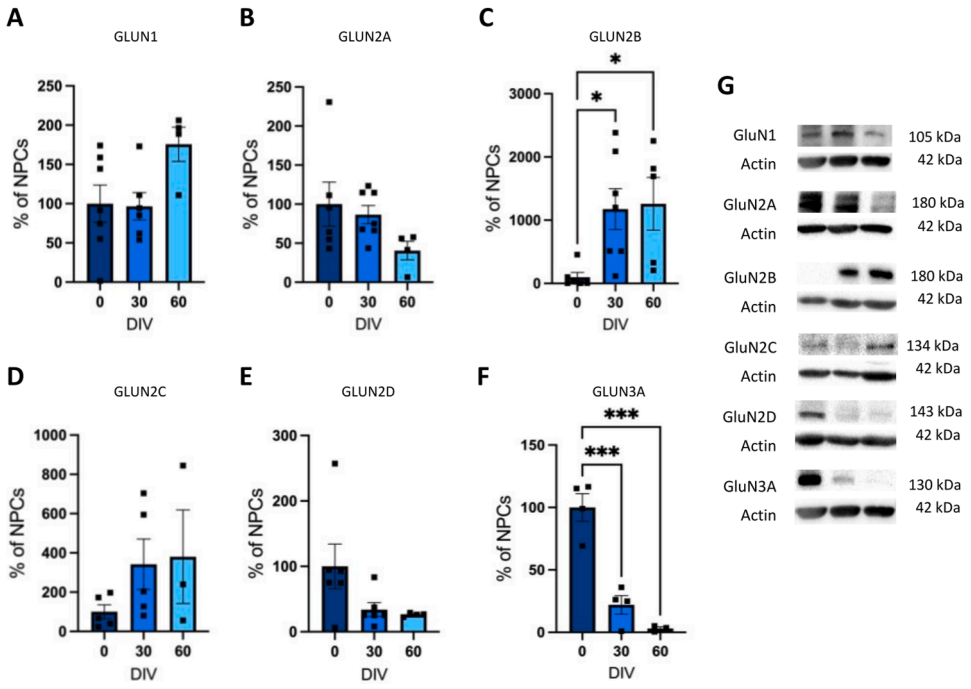

Fig. 5. Protein abundance of the NMDA receptor subunits. Western blot analysis of GluN1 (A), GluN2A (B), GluN2B (C), GluN2C (D), GluN2D (E), and GluN3A (F) at 30 and 60 DIV of hNPCs differentiation. Data are expressed as % of NPCs (0 DIV). Protein levels were normalized to actin and expressed as mean ± SEM ($n \geq 5$). Representative western blot images (G). One-way ANOVA followed by Dunnett's post-hoc test * $p < 0.05$; *** $p < 0.001$.

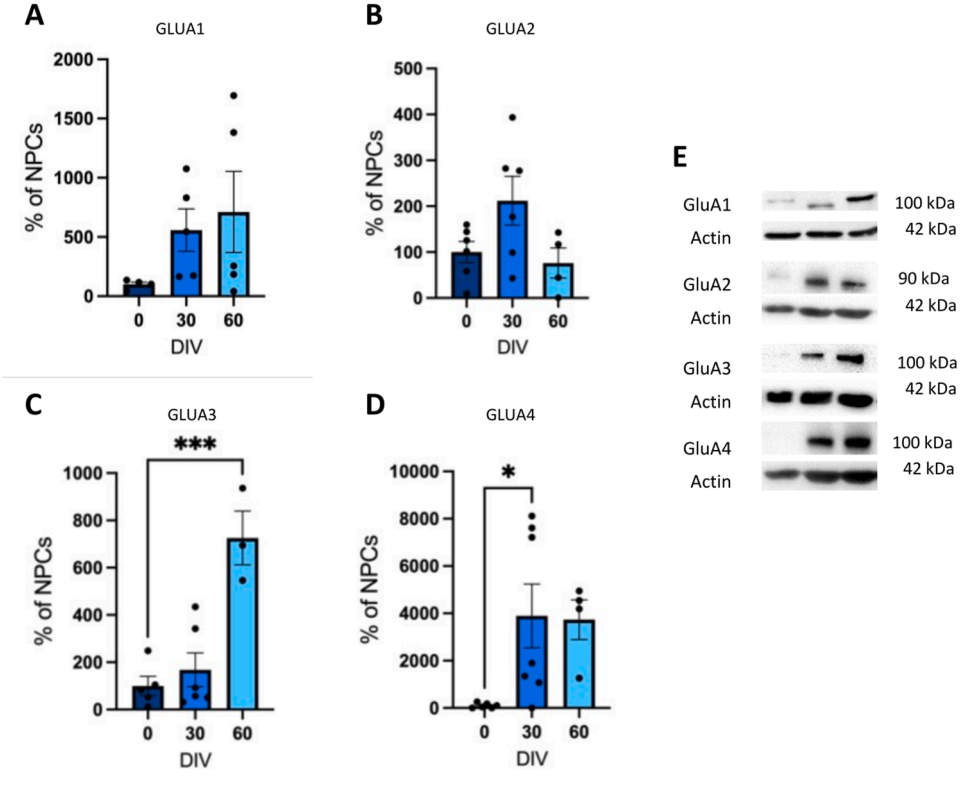

Fig. 6. Protein abundance of the AMPA receptor subunits. Western blot analysis of GluA1 (A), GluA2 (B), GluA3 (C), and GluA4 (D) at 30 and 60 DIV of hNPCs differentiation. Data are expressed as % of NPCs (0 DIV). Protein levels were normalized to actin and expressed as mean ± SEM ($n \geq 5$). Representative western blot images (E). One-way ANOVA followed by Dunnett's post-hoc test * $p < 0.05$; *** $p < 0.001$.

demonstrated the presence of the GluN2A/GluN2B switch in hiPSC-derived ventral mesencephalic neurons at the transcript level (Antonov et al., 2019). Crucially, our in vitro system failed to reproduce this expected GluN2A/GluN2B developmental switch. Despite an

increase in its transcript level, GluN2A protein levels remained low at the analyzed time points. This observation is supported by other studies that have also noted maturational challenges in human iPSC-derived neuronal models. For example, a study by Neagoe et al. (2018) characterized NMDAR subunit expression in human iPSC-derived cortical neurons and found an immature expression profile. Their Western blot analysis revealed a time-dependent increase in GluN1 subunit expression from 3 to 15 DIV, yet GluN2B was the most highly expressed subunit and remained stable. Consistent with an immature phenotype, GluN2A, GluN2C, and GluN2D subunits showed minimal or undetectable protein expression. These molecular findings were further corroborated by electrophysiological analysis using ifenprodil, a selective antagonist for GluN2B-containing receptors, confirming that GluN2B was the predominant subunit underlying NMDA-induced currents (Neagoe et al., 2018). On the contrary, Ruden et al. (2021) demonstrated the presence of all NMDAR subunits in their human forebrain neuron model at 5 weeks of differentiation. Their time-course analysis indicated a potential GluN2B/GluN2A developmental switch, as both mRNA and protein levels for the GluN2A subunit increased at late time points, above 30 DIV, while GluN1 and GluN2B subunits appeared stable. However, this conclusion should be interpreted with caution due to some limitations. The data were from a single time course, lacking statistical power from multiple biological replicates. Furthermore, the term “forebrain-type neurons" is relatively generic, as this broad category encompasses multiple specific brain areas with distinct maturational trajectories. Disse et al. (2023) also demonstrated by RT-qPCR at 8 weeks of differentiation the presence of all NMDA receptor subunits; however, the assay was not quantitative. Moreover, no time course was provided, so expression dynamics at earlier or later stages remain unknown, and no quantitative protein-level analysis was reported. This collection of data, together with ours, suggests that functional NMDAR expression and subunit composition in hiPSC-derived neurons often require an extended culture period beyond 60 DIV or additional maturation cues to emerge (Odawara et al., 2016), highlighting a common challenge in the field. In addition to the peculiar switch between GluN2B and GluN2A subunits of the NMDAR, other subunits also exhibit precise temporal expression patterns. For example, GluN3A expression is known to peak during early development and then sharply decline in mature neurons (Wong et al., 2002; Pérez-Otaño et al., 2006). In our system, we detected an increase in *grin3a* mRNA levels at 30 DIV. Another study reported a similar trend of increased *grin3a* mRNA levels at 4 and 6 weeks, though the authors did not provide information about protein expression (Cheng et al., 2024). Here, our data again revealed a discrepancy between mRNA expression and protein abundance: at both 30 and 60 DIV, the protein levels were significantly lower than those of NPCs at 0 DIV. The GluN3A-containing NMDARs play a role in limiting calcium permeability and synaptic maturation (Corlew et al., 2008; González-González et al., 2023); thus, their removal promotes synaptic maturation while their sustained expression may contribute to immature electrophysiological properties (Roberts et al., 2009).

Similar to NMDARs, during neurodevelopment, AMPARs also change their subunit composition; these are fundamental processes for: excitatory synapse formation and stabilization, synaptic plasticity, and the establishment of neural circuits (Henley and Wilkinson, 2016; Traynelis et al., 2010). Evidence indicates that functional surface AMPARs are expressed by neuronal progenitors (Hagimura et al., 2004). Early synapses predominantly express calcium-permeable AMPARs (Pickard et al., 2000), including GluA1 (Henley and Wilkinson, 2016) and GluA4 (Bassani et al., 2013) subunits. As the CNS matures, a significant shift occurs, leading to the replacement of calcium-permeable AMPARs with calcium-impermeable AMPARs (Pellegrini-Giampietro et al., 1992). In fully developed synapses, AMPARs with GluA4 are replaced by those with GluA2, leading to higher GluA2 expression (Zhu et al., 2000). Moreover, a crucial mechanism is the Q/R modification of the GluA2 subunit, where glutamine (Q) is modified to arginine (R) (Whitney et al., 2008). Q/R editing of GluA2 subunits regulates calcium permeability, with unedited forms allowing higher conductance (Greger et al., 2003). Evidence has been found that, during development, astrocytes can influence the composition and surface expression of synaptic AMPAR subunits by secreting specific factors (Allen, 2013). In rats, almost all AMPAR-positive synapses express GluA2 by postnatal day 14 (Monyer et al., 1991). A similar maturation process occurs in the human brain, although the exact timing may differ across species (Pachernegg et al., 2015). Finally, GluA3 is also expressed, present, though at lower levels compared to GluA1 and GluA2. In our system, we observed several patterns in AMPAR subunit expression. We detected an increase in *gria2* mRNA at 30 DIV, which is consistent with the developmental upregulation of GluA2. This increase in *gria2* mRNA, along with *gria3* mRNA, aligns with the findings of Cheng et al. (2024), who reported a peak expression for these subunits at 4 weeks in hiPSC-derived neurons. For GluA1, our findings of non-significant differences in *gria1* mRNA levels between 0 and 30 DIV contrast with the 4-week peak reported by Cheng and colleagues (Cheng et al., 2024). Our data further revealed a clear uncoupling between mRNA and protein levels for certain subunits. While *gria3* and *gria4* mRNA levels increased at 30 DIV, which was consistent with an increase in their corresponding proteins, GluA3 protein levels showed a delayed increase at 60 DIV, whereas GluA4 was already increased by 30 DIV. Most notably, although the GluA2 protein showed a time-dependent increasing trend, it seemed to return to the levels observed in NPCs by 60 DIV. This suggests that the GluA2-mediated developmental maturation may be incomplete or stalled in our model, further reinforcing the challenges in fully recapitulating synaptic development in a standard in vitro setting.

The discrepancy between transcript and protein levels of glutamatergic receptors is a critical finding that highlights a key challenge in our model: achieving molecular and functional maturity. While our protocol successfully generated neurons, which is consistent with the initial differentiation trajectory (Romito et al., 2024), the lack of a proper developmental switch in NMDARs and AMPARs might suggest that the neuronal population has not reached a fully mature state, with transcriptional programs initiated but not yet translated into functional protein expression. This is further supported by the analysis of pre- and post-synaptic markers, which did not reveal the formation of organized synaptic contacts, suggesting an absence of synaptic maturation. Since the formation of synaptic contacts represents a functional readout of NMDA receptor membrane insertion and maturation, these findings are in line with previous reports, using the same differentiation protocol, which described immature glutamatergic signaling at comparable time points (Romito et al., 2024). Moreover, it is important to acknowledge that the model may not reach full electrophysiological maturity within the tested timeframe. Romito et al. (2024) have shown limited action potential firing and immature passive properties. The acquisition of functional neurotransmitter receptors, together with mature electrophysiological profiles and morphological features like complex neurite arborization, is widely considered a hallmark of neuronal maturity in vitro (Baldassari et al., 2022). Our observations align with other published studies suggesting that functional NMDAR expression might require a longer culture time. For instance, studies have shown that mature synaptic network activity can take over 20–30 weeks to develop (Lepski et al., 2011; Odawara et al., 2016). Environmental conditions also play a key role, with co-culture with astrocytes being shown to enhance synaptogenesis and NMDAR trafficking (Antonov et al., 2019; Autar et al. 2022). While our cultures did contain astrocytic markers (i.e., GFAP), they were generated under feeder-free conditions, which may lack essential trophic support and contribute to the observed inefficient receptor assembly.

These findings have three major implications. First, they suggest that our neuronal population, within the tested time frame, may not be fully suitable for modeling NMDAR-mediated excitotoxicity, a key functional readout in neurotoxicology (Zhou et al., 2013). Second, our results emphasize the importance of model selection and rigorous characterization not only in neurotoxicity studies, but more generally in in vitro

neuroscience research. Substantial variability in receptor composition and function can arise from different differentiation protocols and maturation conditions (Gunhanlar et al., 2018). Third, relying solely on transcriptional profiling may lead to an overestimation of neuronal development. Without comprehensive molecular data, functional validation, particularly through electrophysiological recordings, is essential. The use of selective pharmacological inhibitors targeting individual NMDA and AMPA receptor subunits could offer critical insights into actual receptor expression and synaptic functionality. These strategies help determine whether receptors are not only transcribed, but also translated, assembled, and functionally incorporated into synapses.

Future work should aim to enhance the expression of a complete receptor repertoire, following temporal patterns that better mimic in vivo neurodevelopment. Such efforts are crucial for achieving the functional sophistication required for reliable in vitro models (Masjosthusmann et al., 2020; Bartmann et al., 2023). Accelerated differentiation protocols (e.g., NGN-2 induction) show promise in reducing heterogeneity and improving electrophysiological and synaptic features (Servetti et al., 2025), though challenges such as scalability remain. Comparative studies are needed to identify the most appropriate models for specific toxicological endpoints. Ultimately, our findings underscore the need to validate in vitro models not only by differentiation markers, but by their ability to recapitulate the molecular and functional hallmarks of mature neurons. This is essential for generating reproducible data and ensuring the translational relevance of NAMs in neurotoxicity testing.

CRediT authorship contribution statement

Giacomo Grumelli: Writing – original draft, Visualization, Methodology, Investigation, Formal analysis. **Alessandro Cutarelli:** Writing – review & editing, Methodology. **Marina Marinovich:** Supervision. **Luciano Conti:** Writing – review & editing, Resources. **Barbara Viviani:** Writing – review & editing, Supervision, Project administration, Conceptualization. **Melania Maria Serafini:** Writing – review & editing, Writing – original draft, Visualization, Project administration, Methodology, Investigation, Formal analysis, Data curation, Conceptualization. **Miriam Midali:** Writing – review & editing, Visualization, Methodology, Investigation, Formal analysis, Conceptualization.

Funding

This research received no specific funding.

Declaration of Competing Interest

The authors declare that they have no known competing financial interests or personal relationships that could have appeared to influence the work reported in this paper.

Appendix A. Supporting information

Supplementary data associated with this article can be found in the online version at doi:10.1016/j.toxlet.2026.111834.

Data availability

Data will be made available on request.

References

Acutain, M.F., Griebler Luft, J., Vazquez, C.A., et al., 2021. Reduced expression of hippocampal GluN2A-NMDAR increases seizure susceptibility and causes deficits in contextual memory. Front. Neurosci. 15, 644100. https://doi.org/10.3389/fnins.2021.644100.

Addis, L., Virdee, J.K., Vidler, L.R., Collier, D.A., Pal, D.K., Ursu, D., 2017. Epilepsy-associated GRIN2A mutations reduce NMDA receptor trafficking and agonist potency - molecular profiling and functional rescue. Sci. Rep. 7 (1), 66. https://doi.org/10.1038/s41598-017-00115-w.

Allen, N.J., 2013. Role of glia in developmental synapse formation. Curr. Opin. Neurobiol. 23 (6), 1027–1033. https://doi.org/10.1016/j.conb.2013.06.004.

Amador-Arjona, A., Cimadamore, F., Huang, C.T., et al., 2015. SOX2 primes the epigenetic landscape in neural precursors enabling proper gene activation during hippocampal neurogenesis. Proc. Natl. Acad. Sci. USA 112 (15), E1936–E1945. https://doi.org/10.1073/pnas.1421480112.

Andersen, C.L., Jensen, J.L., Ørntoft, T.F., 2004. Normalization of real-time quantitative reverse transcription-PCR data: a model-based variance estimation approach to identify genes suited for normalization, applied to bladder and colon cancer data sets. Cancer Res. 64 (15), 5245–5250. https://doi.org/10.1158/0008-5472.CAN-04-0496.

Antonov, S.A., Novosadova, E.V., Kobylyansky, A.G., Illarioshkin, S.N., Tarantul, V.Z., Grivennikov, I.A., 2019. Expression and functional properties of NMDA and GABAA receptors during differentiation of human induced pluripotent stem cells into ventral mesencephalic neurons. Biochemistry (Mosc 84 (3), 310–320. https://doi.org/10.1134/S0006297919030131.

Autar, K., Guo, X., Rumsey, J.W., et al., 2022. A functional hiPSC-cortical neuron differentiation and maturation model and its application to neurological disorders. Stem Cell Rep. 17 (1), 96–109. https://doi.org/10.1016/j.stemcr.2021.11.009.

Baldassari, S., Cervetto, C., Amato, S., et al., 2022. Vesicular glutamate release from feeder-FreehiPSC-derived neurons. Int. J. Mol. Sci. 23 (18), 10545. https://doi.org/10.3390/ijms231810545.

Bal-Price, A., Hogberg, H.T., Crofton, K.M., et al., 2018. Recommendation on test readiness criteria for new approach methods in toxicology: exemplified for developmental neurotoxicity. ALTEX 35 (3), 306–352. https://doi.org/10.14573/altex.1712081.

Banker, G., Goslin, K., 1998. Culturing Nerve Cells, 2nd edition. MIT Press.

Barral, S., Kurian, M.A., 2016. Utility of induced pluripotent stem cells for the study and treatment of genetic diseases: focus on childhood neurological disorders. Front. Mol. Neurosci. 9 (78). https://doi.org/10.3389/fnmol.2016.00078.

Bar-Shira, O., Maor, R., Chechik, G., 2015. Gene expression switching of receptor subunits in human brain development. PLoS Comput. Biol. 11 (12), e1004559. https://doi.org/10.1371/journal.pcbi.1004559.

Bartmann, K., Bendt, F., Dönmez, A., et al., 2023. A human iPSC-based in vitro neural network formation assay to investigate neurodevelopmental toxicity of pesticides. ALTEX 40 (3), 452–470. https://doi.org/10.14573/altex.2206031.

Bassani, S., Folci, A., Zapata, J., Passafaro, M., 2013. AMPAR trafficking in synapse maturation and plasticity. Cell Mol. Life Sci. 70 (23), 4411–4430. https://doi.org/10.1007/s00018-013-1309-1.

Belachew, S., Gallo, V., 2004. Synaptic and extrasynaptic neurotransmitter receptors in glial precursors' quest for identity. Glia 48 (3), 185–196. https://doi.org/10.1002/glia.20077.

Bernal, A., Arranz, L., 2018. Nestin-expressing progenitor cells: function, identity and therapeutic implications. Cell Mol. Life Sci. 75 (12), 2177–2195. https://doi.org/10.1007/s00018-018-2794-z.

Berryer, M.H., Rizki, G., Nathanson, A., et al., 2023. High-content synaptic phenotyping in human cellular models reveals a role for BET proteins in synapse assembly. Elife 12, e80168. https://doi.org/10.7554/eLife.80168.

Burnashev, N., Szepetowski, P., 2015. NMDA receptor subunit mutations in neurodevelopmental disorders. Curr. Opin. Pharmacol. 20, 73–82. https://doi.org/10.1016/j.coph.2014.11.008.

Cheng, J.L., Cook, A.L., Talbot, J., Perry, S., 2024. How is excitotoxicity being modelled in iPSC-derived neurons? Neurotox. Res. 42 (5), 43. https://doi.org/10.1007/s12640-024-00721-3.

Cohen-Cory, S., 2002. The developing synapse: construction and modulation of synaptic structures and circuits. Science 298 (5594), 770–776. https://doi.org/10.1126/science.1075510.

Corlew, R., Brasier, D.J., Feldman, D.E., Philpot, B.D., 2008. Presynaptic NMDA receptors: newly appreciated roles in cortical synaptic function and plasticity. Neuroscientist 14 (6), 609–625. https://doi.org/10.1177/1073858408322675.

Disse, P., Aymanns, I., Ritter, N., et al., 2023. A novel NMDA receptor test model based on hiPSC-derived neural cells. Biol. Chem. 404 (4), 267–277. https://doi.org/10.1515/hsz-2022-0216.

European Commission SWD (2024) 185 final ⟨https://environment.ec.europa.eu/topics/chemicals/animals-science_en#related-links⟩ (Accessed on Feb 7, 2025).

European Union 2010 ⟨https://eur-lex.europa.eu/legal-content/EN/TXT/?uri=CELEX%3A02010L0063-20190626⟩ (Accessed on Feb 7, 2025).

FDA, 2025 ⟨www.fda.gov/media/186092/download⟩ (Accessed on August 10, 2025).

Fritsche, E., Crofton, K.M., Hernandez, A.F., et al., 2017. OECD/EFSA workshop on developmental neurotoxicity (DNT): the use of non-animal test methods for regulatory purposes. ALTEX 34 (2), 311–315. https://doi.org/10.14573/altex.1701171.

Fritsche, E., Tigges, J., Hartmann, J., Kapr, J., Serafini, M.M., Viviani, B., 2021. Neural in vitro models for studying substances acting on the central nervous system. Handb. Exp. Pharmacol. 265, 111–141. https://doi.org/10.1007/164_2020_367.

Gambrill, A.C., Barria, A., 2011. NMDA receptor subunit composition controls synaptogenesis and synapse stabilization. Proc. Natl. Acad. Sci. USA 108 (14), 5855–5860. https://doi.org/10.1073/pnas.1012676108.

Gameiro-Ros, I., Tengolics, A.J., Prytkova, I., Kamarajan, C., Pang, Z.P., Goate, A.M., Hart, R.P., Slesinger, P.A., 2025. High-throughput measurements of neuronal activity in single human iPSC-derived glutamate neurons. bioRxiv 04 (07), 646449. https://doi.org/10.1101/2025.04.07.646449.

González-González, I.M., Gray, J.A., Ferreira, J., et al., 2023. GluN3A subunit tunes NMDA receptor synaptic trafficking and content during postnatal brain

development. Cell Rep. 42 (5), 112477. https://doi.org/10.1016/j.celrep.2023.112477.
Greger, I.H., Khatri, L., Kong, X., Ziff, E.B., 2003. AMPA receptor tetramerization is mediated by Q/R editing. Neuron 40 (4), 763–774. https://doi.org/10.1016/s0896-6273(03)00668-8.
Grimm, H., Biller-Andorno, N., Buch, T., et al., 2023. Advancing the 3Rs: innovation, implementation, ethics and society. Front. Vet. Sci. 10, 1185706. https://doi.org/10.3389/fvets.2023.1185706.
Gunhanlar, N., Shpak, G., van der Kroeg, M., et al., 2018. A simplified protocol for differentiation of electrophysiologically mature neuronal networks from human induced pluripotent stem cells. Mol. Psychiatry 23 (5), 1336–1344. https://doi.org/10.1038/mp.2017.56.
Hamada, S., Ogawa, I., Yamasaki, M., Kiyama, Y., Kassai, H., Watabe, A.M., Nakao, K., Aiba, A., Watanabe, M., Manabe, T., 2014. The glutamate receptor GluN2 subunit regulates synaptic trafficking of AMPA receptors in the neonatal mouse brain. Eur. J. Neurosci. 40 (8), 3136–3146. https://doi.org/10.1111/ejn.12682.
Hagimura, N., Tsuzuki, K., Iino, M., et al., 2004. Predominant expression of GluR2 among the AMPA receptor subunits in neuronal progenitor cells of the rat hippocampus. Brain Res. Dev. Brain Res. 152 (2), 213–223. https://doi.org/10.1016/j.devbrainres.2004.07.005.
Harada, A., Teng, J., Takei, Y., Oguchi, K., Hirokawa, N., 2002. MAP2 is required for dendrite elongation, PKA anchoring in dendrites, and proper PKA signal transduction. J. Cell Biol. 158 (3), 541–549. https://doi.org/10.1083/jcb.200110134.
Henley, J.M., Wilkinson, K.A., 2016. Synaptic AMPA receptor composition in development, plasticity and disease. Nat. Rev. Neurosci. 17 (6), 337–350. https://doi.org/10.1038/nrn.2016.37.
Hirbec, H., Déglon, N., Foo, L.C., Goshen, I., Grutzendler, J., Hangen, E., Kreisel, T., Linck, N., Muffat, J., Regio, S., Rion, S., Escartin, C., 2020. Emerging technologies to study glial cells. Glia 68 (9), 1692–1728. https://doi.org/10.1002/glia.23780.
Kaech, S., Banker, G., 2006. Culturing hippocampal neurons. Nat. Protoc. 1 (5), 2406–2415. https://doi.org/10.1038/nprot.2006.356.
Klima, S., Brüll, M., Spreng, A.S., et al., 2021. A human stem cell-derived test system for agents modifying neuronal N-methyl-D-aspartate-type glutamate receptor Ca^{2+}-signalling. Arch. Toxicol. 95 (5), 1703–1722. https://doi.org/10.1007/s00204-021-03024-0.
Kosenkov, A.M., Maiorov, S.A., Gaidin, S.G., 2024. Astrocytic NMDA receptors. Biochemistry (Mosc 89 (6), 1045–1060. https://doi.org/10.1134/S0006297924060063.
Lepski, G., Maciaczyk, J., Jannes, C.E., Maciaczyk, D., Bischofberger, J., Nikkhah, G., 2011. Delayed functional maturation of human neuronal progenitor cells in vitro. Mol. Cell Neurosci. 47 (1), 36–44. https://doi.org/10.1016/j.mcn.2011.02.011.
Li, D., Liu, X., Liu, T., et al., 2020. Neurochemical regulation of the expression and function of glial fibrillary acidic protein in astrocytes. Glia 68 (5), 878–897. https://doi.org/10.1002/glia.23734.
Marei, H.E.S., El-Gamal, A., Althani, A., et al., 2018. Cholinergic and dopaminergic neuronal differentiation of human adipose tissue derived mesenchymal stem cells [published correction appears in J Cell Physiol. 2019 Jul;234(7):12088. doi: 10.1002/jcp.28150.]. J. Cell Physiol. 233 (2), 936–945. https://doi.org/10.1002/jcp.25937.
Masjosthusmann, S., Blum, J., Bartmann, K., et al., 2020. Establishment of an a priori protocol for the implementation and interpretation of an in-vitro testing battery for the assessment of developmental neurotoxicity. EFSA Support. Publ. 17 (10), EN-1938. https://doi.org/10.2903/sp.efsa.2020.EN-1938.
Mateos-Aparicio, P., Bello, S.A., Rodríguez-Moreno, A., 2020. Challenges in physiological phenotyping of hiPSC-derived neurons: from 2D cultures to 3D brain organoids. Front. Cell Dev. Biol. 8, 797. https://doi.org/10.3389/fcell.2020.00797.
Monyer, H., Seeburg, P.H., Wisden, W., 1991. Glutamate-operated channels: developmentally early and mature forms arise by alternative splicing. Neuron 6 (5), 799–810. https://doi.org/10.1016/0896-6273(91)90176-z.
Neagoe, I., Liu, C., Stumpf, A., et al., 2018. The GluN2B subunit represents a major functional determinant of NMDA receptors in human induced pluripotent stem cell-derived cortical neurons. Stem Cell Res. 28, 105–114. https://doi.org/10.1016/j.scr.2018.02.002.
Nimtz, L., Hartmann, J., Tigges, J., et al., 2020. Characterization and application of electrically active neuronal networks established from human induced pluripotent stem cell-derived neural progenitor cells for neurotoxicity evaluation. Stem Cell Res. 45, 101761. https://doi.org/10.1016/j.scr.2020.101761.
Niwa, S., Takahashi, H., Hirokawa, N., 2013. β-Tubulin mutations that cause severe neuropathies disrupt axonal transport. EMBO J. 32 (10), 1352–1364. https://doi.org/10.1038/emboj.2013.59.
Odawara, A., Katoh, H., Matsuda, N., Suzuki, I., 2016. Physiological maturation and drug responses of human induced pluripotent stem cell-derived cortical neuronal networks in long-term culture. Sci. Rep. 6, 26181. https://doi.org/10.1038/srep26181.
OECD, 2023. Initial Recommendations on Evaluation of Data from the Developmental Neurotoxicity (DNT) In-Vitro Testing Battery, OECD Series on Testing and Assessment, No. 377. OECD Publishing, Paris. https://doi.org/10.1787/91964ef3-en.
Pachernegg, S., Münster, Y., Muth-Köhne, E., Fuhrmann, G., Hollmann, M., 2015. GluA2 is rapidly edited at the Q/R site during neural differentiation in vitro. Front. Cell Neurosci. 9 (69). https://doi.org/10.3389/fncel.2015.00069.
Paoletti, P., Bellone, C., Zhou, Q., 2013. NMDA receptor subunit diversity: impact on receptor properties, synaptic plasticity and disease. Nat. Rev. Neurosci. 14 (6), 383–400. https://doi.org/10.1038/nrn3504.
Pellegrini-Giampietro, D.E., Bennett, M.V., Zukin, R.S., 1992. Are Ca(2+)-permeable kainate/AMPA receptors more abundant in immature brain? Neurosci. Lett. 144 (1-2), 65–69. https://doi.org/10.1016/0304-3940(92)90717-l.
Pérez-Otaño, I., Luján, R., Tavalin, S.J., et al., 2006. Endocytosis and synaptic removal of NR3A-containing NMDA receptors by PACSIN1/syndapin1. Nat. Neurosci. 9 (5), 611–621. https://doi.org/10.1038/nn1680.
Pevny, L.H., Sockanathan, S., Placzek, M., Lovell-Badge, R., 1998. A role for SOX1 in neural determination. Development 125 (10), 1967–1978. https://doi.org/10.1242/dev.125.10.1967.
Pfaffl, M.W., Tichopad, A., Prgomet, C., Neuvians, T.P., 2004. Determination of stable housekeeping genes, differentially regulated target genes and sample integrity: BestKeeper–Excel-based tool using pair-wise correlations. Biotechnol. Lett. 26 (6), 509–515. https://doi.org/10.1023/b:bile.0000019559.84305.47.
Pickard, L., Noël, J., Henley, J.M., Collingridge, G.L., Molnar, E., 2000. Developmental changes in synaptic AMPA and NMDA receptor distribution and AMPA receptor subunit composition in living hippocampal neurons. J. Neurosci. 20 (21), 7922–7931. https://doi.org/10.1523/JNEUROSCI.20-21-07922.2000.
Poh, W.T., Stanslas, J., 2024. The new paradigm in animal testing – "3Rs alternatives". Regul. Toxicol. Pharmacol. 153, 105705. https://doi.org/10.1016/j.yrtph.2024.105705. ISSN 0273-2300.
Rao, A., Craig, A.M., 1997. Activity regulates the synaptic localization of the NMDA receptor in hippocampal neurons. Neuron 19 (4), 801–812. https://doi.org/10.1016/s0896-6273(00)80962-9.
Rice, D., Barone, S.Jr, 2000. Critical periods of vulnerability for the developing nervous system: evidence from humans and animal models. Environ. Health Perspect. 108 (Suppl 3), 511–533. https://doi.org/10.1289/ehp.00108s3511.
Roberts, A.C., Díez-García, J., Rodriguiz, R.M., et al., 2009. Downregulation of NR3A-containing NMDARs is required for synapse maturation and memory consolidation. Neuron 63 (3), 342–356. https://doi.org/10.1016/j.neuron.2009.06.016.
Rodier, P.M., 1994. Vulnerable periods and processes during central nervous system development. Environ. Health Perspect. 102 (Suppl 2), 121–124. https://doi.org/10.1289/ehp.94102121.
Romito, E., Battistella, I., Plakhova, V., et al., 2024. A comprehensive protocol for efficient differentiation of human NPCs into electrically competent neurons. J. Neurosci. Methods 410, 110225. https://doi.org/10.1016/j.jneumeth.2024.110225.
Ruden, J.B., Dixit, M., Zepeda, J.C., Grueter, B.A., Dugan, L.L., 2021. Robust expression of functional NMDA receptors in human induced pluripotent stem cell-derived neuronal cultures using an accelerated protocol. Front. Mol. Neurosci. 14, 777049. https://doi.org/10.3389/fnmol.2021.777049.
Russell, W.M.S., Burch, R.L., 1959. The Principles of Humane Experimental Technique Methuen.
Sachana, M., Bal-Price, A., Crofton, K.M., et al., 2019. International regulatory and scientific effort for improved developmental neurotoxicity testing. Toxicol. Sci. 167 (1), 45–57. https://doi.org/10.1093/toxsci/kfy211.
Sansom, S.N., Griffiths, D.S., Faedo, A., et al., 2009. The level of the transcription factor Pax6 is essential for controlling the balance between neural stem cell self-renewal and neurogenesis. PLoS Genet. 5 (6), e1000511. https://doi.org/10.1371/journal.pgen.1000511.
Sanz-Clemente, A., Nicoll, R.A., Roche, K.W., 2013. Diversity in NMDA receptor composition: many regulators, many consequences. Neuroscientist 19 (1), 62–75. https://doi.org/10.1177/1073858411435129.
Serafini, M.M., Sepehri, S., Midali, M., et al., 2024. Recent advances and current challenges of new approach methodologies in developmental and adult neurotoxicity testing. Arch. Toxicol. 98 (5), 1271–1295. https://doi.org/10.1007/s00204-024-03703-8.
Servetti, M., Caramia, M., Parodi, G., et al., 2025. Optimization of transcription factor-driven neuronal differentiation from human induced pluripotent stem cells for disease modelling and drug screening. Stem Cell Rev. Rep. 21 (3), 816–833. https://doi.org/10.1007/s12015-025-10845-4.
Shipton, O.A., Paulsen, O., 2013. GluN2A and GluN2B subunit-containing NMDA receptors in hippocampal plasticity. Philos. Trans. R. Soc. Lond. B Biol. Sci. 369 (1633), 20130163. https://doi.org/10.1098/rstb.2013.0163.
Singh, N., Siebzehnrubl, F.A., Martinez-Garay, I., 2023. Transcriptional control of embryonic and adult neural progenitor activity. Front. Neurosci. 17, 1217596. https://doi.org/10.3389/fnins.2023.1217596.
Storey, G.P., Riquelme, R., Barria, A., 2025. Activity-dependent internalization of Glun2B-containing NMDARs is required for synaptic incorporation of Glun2A and synaptic plasticity. J. Neurosci. 45 (4), e0823242024. https://doi.org/10.1523/JNEUROSCI.0823-24.2024.
Szabo, A., Akkouh, I.A., Vandenberghe, M., et al., 2021. A human iPSC-astroglia neurodevelopmental model reveals divergent transcriptomic patterns in schizophrenia. Transl. Psychiatry 11 (1), 554. https://doi.org/10.1038/s41398-021-01681-4.
Tal, T., Myhre, O., Fritsche, E., et al., 2024. New approach methods to assess developmental and adult neurotoxicity for regulatory use: a PARC work package 5 project. Front. Toxicol. 6, 1359507. https://doi.org/10.3389/ftox.2024.1359507.
Telias, M., 2023. Neural differentiation protocols: how to choose the correct approach. Neural Regen. Res. 18 (6), 1273–1274. https://doi.org/10.4103/1673-5374.360171.
Törnqvist, E., Annas, A., Granath, B., Jalkesten, E., Cotgreave, I., Öberg, M., 2014. Strategic focus on 3R principles reveals major reductions in the use of animals in pharmaceutical toxicity testing. PLoS One 9 (7). https://doi.org/10.1371/journal.pone.0101638.

Traynelis, S.F., Wollmuth, L.P., McBain, C.J., et al., 2010. Glutamate receptor ion channels: structure, regulation, and function. Pharmacol. Rev. 62 (3), 405–496. https://doi.org/10.1124/pr.109.002451.

Tumdam, R., Hussein, Y., Garin-Shkolnik, T., Stern, S., 2024. NMDA receptors in neurodevelopmental disorders: pathophysiology and disease models. Int. J. Mol. Sci. 25 (22), 12366. https://doi.org/10.3390/ijms252212366.

Uzunova, G., Hollander, E., Shepherd, J., 2014. The role of ionotropic glutamate receptors in childhood neurodevelopmental disorders: autism spectrum disorders and fragile x syndrome. Curr. Neuropharmacol. 12 (1), 71–98. https://doi.org/10.2174/1570159X113116660046.

Verkhratsky, A., Chvátal, A., 2020. NMDA receptors in astrocytes. Neurochem. Res. 45 (1), 122–133. https://doi.org/10.1007/s11064-019-02750-3.

Vieira, M.M., Nguyen, T.A., Wu, K., Badger, J.D., 2nd, Collins, B.M., Anggono, V., Lu, W., Roche, K.W., 2020. An epilepsy-associated GRIN2A rare variant disrupts CaMKIIα phosphorylation of GluN2A and NMDA receptor trafficking. Cell Rep. 32 (9), 108104. https://doi.org/10.1016/j.celrep.2020.108104.

Vieira, M.M., Peng, S., Won, S., Hong, E., Inati, S.K., Thurm, A., Thiam, A.H., Kim, S., Myers, S.J., Badger, J.D., 2nd, Traynelis, S.F., Lu, W., Roche, K.W., 2024. A frameshift variant of GluN2A identified in an epilepsy patient results in NMDA receptor mistargeting. J. Neurosci. 44 (4), e0557232023. https://doi.org/10.1523/JNEUROSCI.0557-23.2023.

Vyklicky, V., Korinek, M., Smejkalova, T., et al., 2014. Structure, function, and pharmacology of NMDA receptor channels. Physiol. Res. 63 (1), S191–S203. https://doi.org/10.33549/physiolres.932678.

Wegner, M., Stolt, C.C., 2005. From stem cells to neurons and glia: a Soxist's view of neural development. Trends Neurosci. 28 (11), 583–588. https://doi.org/10.1016/j.tins.2005.08.008.

Whitney, N.P., Peng, H., Erdmann, N.B., Tian, C., Monaghan, D.T., Zheng, J.C., 2008. Calcium-permeable AMPA receptors containing Q/R-unedited GluR2 direct human neural progenitor cell differentiation to neurons. FASEB J. 22 (8), 2888–2900. https://doi.org/10.1096/fj.07-104661.

Williams, K., Russell, S.L., Shen, Y.M., Molinoff, P.B., 1993. Developmental switch in the expression of NMDA receptors occurs in vivo and in vitro. Neuron 10 (2), 267–278. https://doi.org/10.1016/0896-6273(93)90317-k.

Wong, H.K., Liu, X.B., Matos, M.F., et al., 2002. Temporal and regional expression of NMDA receptor subunit NR3A in the mammalian brain. J. Comp. Neurol. 450 (4), 303–317. https://doi.org/10.1002/cne.10314.

Yasuda, H., Mukai, H., 2015. Turning off of GluN2B subunits and turning on of CICR in hippocampal LTD induction after developmental GluN2 subunit switch. Hippocampus 25 (11), 1274–1284. https://doi.org/10.1002/hipo.22435.

Yong, X.L.H., Zhang, L., Yang, L., Chen, X., Tan, J.Z.A., Yu, X., Chandra, M., Livingstone, E., Widagdo, J., Vieira, M.M., Roche, K.W., Lynch, J.W., Keramidas, A., Collins, B.M., Anggono, V., 2021. Regulation of NMDA receptor trafficking and gating by activity-dependent CaMKIIα phosphorylation of the GluN2A subunit. Cell Rep. 36 (1), 109338. https://doi.org/10.1016/j.celrep.2021.109338.

Zhou, X., Hollern, D., Liao, J., Andrechek, E., Wang, H., 2013. NMDA receptor-mediated excitotoxicity depends on the coactivation of synaptic and extrasynaptic receptors. Cell Death Dis. 4 (3), e560. https://doi.org/10.1038/cddis.2013.82.

Zhu, J.J., Esteban, J.A., Hayashi, Y., Malinow, R., 2000. Postnatal synaptic potentiation: delivery of GluR4-containing AMPA receptors by spontaneous activity. Nat. Neurosci. 3 (11), 1098–1106. https://doi.org/10.1038/80614.